Nuclear isospin asymmetry in α decay of heavy nuclei

Eunkyoung Shin,[1,*] Yeunhwan Lim,[2,†] Chang Ho Hyun,[3,‡] and Yongseok Oh[1,4,§]
[1]*Department of Physics, Kyungpook National University, Daegu 41566, Korea*
[2]*Rare Isotope Science Project, Institute for Basic Science, Daejeon 34047, Korea*
[3]*Department of Physics Education, Daegu University, Gyeongsan, Gyeongbuk 38453, Korea*
[4]*Asia Pacific Center for Theoretical Physics, Pohang, Gyeongbuk 37673, Korea*
(Received 11 November 2015; revised manuscript received 20 June 2016; published 12 August 2016)

The effects of nuclear isospin asymmetry on α-decay lifetimes of heavy nuclei are investigated within various phenomenological models of the nuclear potential for the α particle. We consider the widely used simple square-well potential and Woods-Saxon potential and modify them by including an isospin asymmetry term. We then suggest a model for the potential of the α particle motivated by a microscopic phenomenological approach of the Skyrme force model, which naturally introduces the isospin-dependent form of the nuclear potential for the α particle. The empirical α-decay lifetime formula of Viola and Seaborg [J. Inorg. Nucl. Chem. **28**, 741 (1966)] is also modified to include isospin asymmetry effects. The obtained α-decay half-lives are in good agreement with the experimental data, and we find that including the nuclear isospin effects somehow improves the theoretical results for α-decay half-lives. The implications of these results are discussed, and the predictions on the α-decay lifetimes of superheavy elements are also presented.

DOI: 10.1103/PhysRevC.94.024320

I. INTRODUCTION

The nuclear α decay has been one of the most important tools to study nuclear forces and nuclear structure [1]. Even today, its role cannot be overemphasized in the investigation of nuclear properties and, in particular, in identifying syntheses of new elements. (See, for example, Refs. [2,3].) Although many facets of the nuclear force were uncovered and understood, there still remain a lot of questions to be explored. One very naive but quite nontrivial question would be how many nucleons can aggregate in the heaviest nucleus? Since every nucleus is dynamical and the α decay is one of the major decay processes of heavy nuclei, the investigation of α decays of superheavy elements is required to find a clue to answer this question.

The structures of superheavy elements and their syntheses have been exciting research topics in both experimental and theoretical nuclear physics [4]. These topics attract recent research interests thanks to the construction of new facilities of rare isotope beams, which will allow the investigation of very neutron-rich nuclei as well as superheavy elements. The stability of nuclei can be achieved through the balance between the attractive nuclear force and the repulsive Coulomb force. As the number of protons increases, the Coulomb repulsion increases, thus more neutrons are required to form a bound state. However, the energy of neutron-rich nuclear matter is higher than that of symmetric nuclear matter because of the nuclear symmetry energy contribution to the total energy. Therefore, the nuclear symmetry energy is important to understand the structure of heavy, in particular, very neutron-rich nuclei [5]. Furthermore, unstable heavy nuclei eventually decay through spontaneous fission, β decay, nucleon, and α emissions, so the role of nuclear symmetry energy or the change in nuclear potential due to nuclear isospin asymmetry in these decay processes deserves to be studied.

In the standard approach, the α-decay lifetimes are governed by the effective potential for the nuclear force which combines the core nucleus and the α cluster. There are several phenomenological potential models for explaining the measured data of α-decay lifetimes, which include the simple α-cluster model with a square-well (SW) potential model [6,7], cosh-type potential model [8], generalized liquid droplet model (GLDM) [9,10], and density-dependent M3Y effective interaction [11–13]. In the simple cluster model, the α particle is trapped by the core nucleus in a nuclear plus Coulomb potential, and the α decay happens as the bound α particle escapes from the potential barrier by quantum tunneling. The shape of the effective nuclear potential felt by the α particle is determined by fitting the parameters of the potential to the measured α-decay lifetimes. Despite its simplicity, these models are quite successful to describe α-decay lifetimes even quantitatively [6,7]. For a more complete description of the data, one, of course, needs to develop more realistic potential models for the α particle.

Improvement of simple potential models has been pursued in several ways. For example, in the simple potential models illustrated above, the shape of a nucleus is robust and does not change during the decay process. Therefore, more realistic treatment on the shape evolution was anticipated and investigated, e.g., in the GLDM in Refs. [9,10]. On the other hand, it is also desirable to understand the α potential in nuclear matter from a microscopic approach. Along this direction, the authors of Refs. [11–13] parametrized the α-particle potential using three Yukawa-type finite-range forces that are modified by nuclear density. In this approach, it is assumed that the core nucleus follows the Fermi density profile and the α particle has the Gaussian density profile.

*shinek@knu.ac.kr
†ylim9057@ibs.re.kr
‡hch@daegu.ac.kr
§yohphy@knu.ac.kr

In the present paper, we explore the nuclear isospin asymmetry effects in the α-decay half-lives of heavy nuclei. The α potential depth depends on isospin asymmetry [14,15], and the potential depth from isospin asymmetry effects is naturally embedded when the double-folding model is employed [11–13]. The effects of the nuclear symmetry energy, i.e., the nuclear isospin asymmetry effects, were also considered in the computation of the Q value of the emergent α particle in Refs. [16,17]. But the nuclear symmetry energy can affect the α-decay lifetimes also through the nuclear potential of the α particle. Therefore, it would be legitimate to investigate the effects of the nuclear symmetry energy on α-decay lifetimes through the modifications of the effective potential of the α particle, which may affect, in particular, the α-decay half-lives of neutron-rich nuclei. We will address this issue in the present paper.

Recent progress shows that the nuclear symmetry energy is well constrained both by experimental data and by theoretical calculations at least near the normal nuclear density, and its effects have been investigated widely in various physical quantities of systems from nuclei to neutron stars [5,18–22]. Since far neutron-rich nuclei play a crucial role in the understanding of the exotic nuclear structure, it is important to see how the nuclear symmetry energy affects the α-decay lifetimes [5]. In principle, therefore, the nuclear symmetry energy should be considered in developing the effective α potential. Instead of invoking a complex microscopic calculation, however, we revisit the simple cluster model and modify the α-particle potential by including the isospin asymmetry term. The model parameters are then fitted to the existing experimental data, and they are used to predict the lifetimes of unknown elements. For a model based on the more microscopic approach we also suggest a potential as a functional of proton and neutron densities relying on the Skyrme force model. In this approach, the isospin asymmetry effects affect both nuclear potential and proton distribution so the penetration length depends on the unequal number of neutrons and protons. Compared with the Yukawa-type finite-range double-folding model [11–13], our approach is based on the zero-range nuclear force (see the Appendix). Finally, we will discuss the modification of the empirical formula of Viola and Seaborg (VS) for α-decay lifetimes by explicitly including the isospin asymmetry term.

This paper is organized as follows. In Sec. II, we discuss the general features of the potential model for nuclear α decay. To investigate the nuclear isospin asymmetry effects, we first consider the square-well potential and the Woods-Saxon (WS) potential and then suggest a potential motivated by the Skyrme force model before we discuss the modification of the empirical Viola-Seaborg formula. The computed α-decay lifetimes of the heavy nuclei of $Z = 106$–118 are compared with existing experimental data in Sec. III. We also present the predictions of α-decay half-lives for superheavy elements in the range of $Z = 117$–122. Section IV contains the summary and a discussion.

II. MODELS OF α DECAY

In this section, we briefly review and introduce potential models for the α particle. The fitting process to find the values of the potential parameters is also shortly described.

A. General features

In the present paper, with a given model potential, we make use of the Wentzel-Kramers-Brillouin (WKB) approximation to calculate the α-decay half-lives of heavy nuclei. In the α-cluster model, the α particle interacts with the core nucleus, which becomes the daughter nucleus after decay, through the strong nuclear interaction and Coulomb interaction. Even though the α particle has a finite size ($r_\alpha \sim 2.0$ fm), it is negligibly small since its volume fraction to the decaying nucleus, or mother nucleus, is less than $1/25$ if $A \geqslant 100$. This justifies the approximation of treating the α particle as an elementary particle, and the α decay can be described by the quantum tunneling of a pointlike particle. The potential of the α particle produced by the core nucleus can be written as

$$V_\alpha(r) = V_N(r) + V_C(r) + V_L(r), \tag{1}$$

where $V_N(r)$ is the nuclear potential, $V_C(r)$ is the Coulomb potential, and $V_L(r)$ is the centrifugal barrier. The explicit forms of each potential are model dependent and will be discussed later in this section.

In the semiclassical approximation [6], the half-life is computed as

$$T_{1/2} = \frac{\hbar \ln 2}{\Gamma}, \tag{2}$$

with [23]

$$\Gamma = \mathcal{P}\mathcal{F}\frac{\hbar^2}{4m_\mu}\exp\left[-2\int_{r_2}^{r_3} dr\, k(r)\right], \tag{3}$$

where m_μ is the reduced mass of the system and $\mathcal{P}$ is the α-particle preformation probability. It is the probability that an α particle is formed inside a nucleus so that the α decay is described as the emission of the preformed α particle. It is understood to be similar to the spectroscopic factor of protons in the case of the proton emission process [24]. Since our purpose is to see the effects of nuclear isospin asymmetry in the nuclear potential of the α particle and the parameters of the potential will be fitted by experimental data, we simply assume $\mathcal{P} = 1$ throughout this paper. The normalization factor $\mathcal{F}$ is defined by

$$\mathcal{F}\int_{r_1}^{r_2}\frac{dr}{k(r)}\cos^2\left[\int_{r_1}^{r_2} dr' k(r') - \frac{\pi}{4}\right] = 1. \tag{4}$$

Physically, $\mathcal{F}$ is the assaulting frequency of the α particle to the potential well by the core nucleus. Here, r_1, r_2, and r_3 denote classical turning points at the centrifugal barrier and inner and outer barriers of the Coulomb potential, respectively. The wave number of the α particle is given by

$$k(r) = \sqrt{\frac{2m_\mu}{\hbar^2}|Q_\alpha - V(r)|}, \tag{5}$$

where Q_α is the energy of the system during the decay process. It is known that the α-decay half-lives are very sensitive to the value of Q_α.

To compute the α-decay half-life, one has to model the potential appearing in Eq. (1). The potentials to model the interaction between the α particle and the core nucleus are parametrized, and these parameters are determined by the

Monte Carlo method with which we minimize the root-mean-square (rms) deviation σ defined as

$$\sigma = \sqrt{\frac{1}{N_{\rm data}-1}\sum\left(\log_{10}\frac{T_{1/2}^{\rm Theory}}{T_{1/2}^{\rm Expt.}}\right)^2}, \tag{6}$$

where $N_{\rm data}$ is the total number of data. In the present paper, we consider three models for the potential and explore a possible modification of the empirical Viola-Seaborg formula for α-decay half-lives.

B. Square-well potential for the α particle

We first consider the square-well potential as the simplest choice for the nuclear potential of the α particle. In Ref. [6], it was found that the square-well potential approach is quite successful to explain the α-decay half-lives considering its simplicity. The square-well potential assumes that nuclei have sharp edges as in the liquid drop model. Since a uniform density is assumed, the nuclear potential for the α particle is constant and attractive. Therefore, we have

$$V_N(r) = \begin{cases} V_0 & \text{for } r < R, \\ 0 & \text{for } r \geqslant R, \end{cases} \tag{7}$$

where R is the radius of the core nucleus and $V_0 < 0$. Since our aim is to explore the effects of the nuclear isospin asymmetry, we just follow the square-well potential model of Refs. [6,7], which assumes the Coulomb potential of the surface charge form as

$$V_C(r) = \begin{cases} \dfrac{Z_1 Z_2 e^2}{R}, & \text{if } r < R, \\ \dfrac{Z_1 Z_2 e^2}{r}, & \text{if } r \geqslant R, \end{cases} \tag{8}$$

where $Z_1 = 2$ and $Z_2 = Z - 2$ in our case. The radius R of the core nucleus is found from the Bohr-Sommerfeld quantization condition,

$$\int_{r_1}^{r_2} dr\, k(r) = \left(n + \frac{1}{2}\right)\pi = (G - \ell + 1)\frac{\pi}{2}, \tag{9}$$

where the value of G depends on the neutron number N as [6,7]

$$G = \begin{cases} 20 & \text{for } N \leqslant 82, \\ 22 & \text{for } 82 < N \leqslant 126, \\ 24 & \text{for } 126 < N. \end{cases} \tag{10}$$

The centrifugal barrier is written as

$$V_L = \frac{\hbar^2}{2m_\mu r^2}\ell(\ell+1), \tag{11}$$

where ℓ is the relative orbital angular momentum between the core nucleus and the α particle. In this calculation, $\ell = 0$ is assumed as in Refs. [6,7], and thus there is no contribution from V_L.[1]

On top of this model, we consider the effects of the nuclear symmetry energy. In order to take into account the isospin asymmetry effects, we modify the α-particle nuclear potential for $r < R$ as

$$V_N(r) = V_0 + V_1 I + V_2 I^2, \tag{12}$$

where

$$I = (N - Z)/A = (N - Z)/(N + Z), \tag{13}$$

with Z being the number of protons so that $A = N + Z$. The constants V_1 and V_2 control the dependence of the nuclear potential on the isospin asymmetry.

C. Woods-Saxon potential for the α particle

More realistic potentials than the simplest square-well potential can be constructed by considering nonuniform distribution of nucleons in the core nucleus. One typical example is the Woods-Saxon potential [25] which assumes Fermi or logistic function distribution of the nucleon density profile. This leads to the nuclear potential in the Woods-Saxon form

$$V_N(r) = \frac{V_0}{1 + \exp[(r - R)/a]}, \tag{14}$$

where R is the rough radius of the nucleus and a is diffuseness parameter. As in the case of the square-well potential model in the previous subsection, the radius R is determined by the quantization condition of Eq. (9). To take into account isospin asymmetry, we modify $V_N(r)$ as [14,15,26][2]

$$V_N(r) = \frac{1}{1 + \exp[(r - R)/a]}(V_0 + V_1 I + V_2 I^2). \tag{15}$$

The value of a obtained from the least σ fitting is found to be $a = 0.4$ fm.[3] We also tried to improve the fitting by allowing the functional form of $a = a(I)$, but it does not show any apparent isospin dependence in minimizing the rms deviation. Thus, we fix $a = 0.4$ fm in our simulation as in Ref. [8].

In this model, the core nucleus is assumed to have a uniform charge distribution [8]. Therefore, unlike the square-well potential model, we have

$$V_C(r) = \begin{cases} \dfrac{Z_1 Z_2 e^2}{2R}\left[3 - \left(\frac{r}{R}\right)^2\right] & \text{for } r < R, \\ \dfrac{Z_1 Z_2 e^2}{r} & \text{for } r \geqslant R. \end{cases} \tag{16}$$

Furthermore, it is known that the proper application of the WKB formula needs to replace V_L by the modified centrifugal barrier of Langer [28], which reads

$$V_L(r) = \frac{\hbar^2}{2m_\mu r^2}\left(\ell + \frac{1}{2}\right)^2. \tag{17}$$

[1] However, as will be discussed in Sec. III, the assumption of $\ell = 0$ is too crude and gives reasonable results only for even-even nuclei.

[2] We thank the referee for pointing out that the nuclear potential may also include the linear term of I.

[3] In Fermi density distribution, the surface diffuseness a is roughly $t_{90\text{-}10}/4.4$, where $t_{90\text{-}10}$ is the radial distance between 90% and 10% of the density peak. For example, $t_{90\text{-}10}$ thickness for ^{208}Pb from the SLy4 Hartree-Fock calculation is about 2.60 fm, which then gives $a \approx 0.59$ fm [27]. This value differs from the fitted value by a factor of 1.5.

In the present study, we vary the angular momentum in the effective α potential to obtain the best fit with the experimental data but with the constraint of parity conservation. This completes our second model for the α potential, and the parameters are determined by minimizing the rms deviation defined in Eq. (6).

D. Potential based on the Skyrme energy density functional

Although the previous two models are based on macroscopic approaches to the nuclear potential of the α particle, the phenomenological Skyrme force model gives a tool based on a more microscopic background to understand the form of the nuclear potential. Within this approach the potentials of protons and neutrons in nuclei are expressed as functions of proton and neutron densities [29].

As in the previous models, we assume that the α particle is small enough to be treated as a pointlike particle. Then a pointlike α particle in a decaying nucleus interacts with pointlike nucleons in the core nucleus. At the leading-order approximation, two-body interactions describe the interactions between the α particle and the nucleons of the core nucleus. Employing the standard form of the energy density functional (EDF) of the Skyrme force, we write the interaction of the α particle as

$$\begin{aligned} v_{N\alpha}(\boldsymbol{k},\boldsymbol{k}') = {} & s_0(1+v_0P_\sigma)\delta(\boldsymbol{r}_{N\alpha}) \\ & + \frac{s_1}{2}(1+v_1P_\sigma)[\delta(\boldsymbol{r}_{N\alpha})\boldsymbol{k}^2 + \boldsymbol{k}'^2\delta(\boldsymbol{r}_{N\alpha})] \\ & + s_2\boldsymbol{k}'\cdot\delta(\boldsymbol{r}_{N\alpha})\boldsymbol{k} + iW_0^\alpha\boldsymbol{k}'\cdot(\boldsymbol{\sigma}\times\boldsymbol{k})\delta(\boldsymbol{r}_{N\alpha}) \\ & + \frac{s_3}{6}(1+v_3P_\sigma)\rho_N^\epsilon\delta(\boldsymbol{r}_{N\alpha}), \end{aligned} \tag{18}$$

where $\boldsymbol{r}_{N\alpha} = \boldsymbol{r}_N - \boldsymbol{r}_\alpha$, $\rho_N = \rho_n + \rho_p$ is the nucleon density, P_σ is the spin-exchange operator, and s_i, v_i, W_0^α, and ϵ are the parameters of the potential. The momenta $\boldsymbol{k}$ and $\boldsymbol{k}'$ are defined as[4]

$$\boldsymbol{k} = \frac{1}{2i}(\nabla_N - \nabla_\alpha), \quad \boldsymbol{k}' = -\frac{1}{2i}(\nabla'_N - \nabla'_\alpha). \tag{19}$$

Evaluating the matrix elements of Eq. (18) leads to a form of the α-particle potential as a functional of the proton and neutron densities as

$$\begin{aligned} V_N = {} & \alpha\rho_N + \beta\left(\rho_n^{5/3} + \rho_p^{5/3}\right) + \gamma\rho_N^\epsilon\left(\rho_N^2 + 2\rho_n\rho_p\right) \\ & + \delta\frac{\rho'_N}{r} + \eta\rho''_N, \end{aligned} \tag{20}$$

where $\rho'_N = d\rho_N/dr$ and $\rho''_N = d^2\rho_N/dr^2$. Details for the derivation of Eq. (20) are described in the Appendix.

As for the density profiles of protons and neutrons, we assume the Fermi distribution, i.e., the form of the logistic function as

$$\begin{aligned} \rho_n &= \frac{\rho_n^0}{1+\exp[(r-R_n)/a_n]}, \\ \rho_p &= \frac{\rho_p^0}{1+\exp[(r-R_p)/a_p]}, \end{aligned} \tag{21}$$

where R_n, R_p are to be determined not from the quantization condition but from the number of neutrons and protons in the core nucleus. We use the values of ρ_n^0, ρ_p^0, a_n, and a_p from the Thomas-Fermi calculation using the SLy4 force. Since the proton distribution is given explicitly, the Coulomb potential can be calculated as

$$V_C(r) = 4\pi Z_1 e^2\left[\frac{1}{r}\int_0^r r'^2\rho_p(r')dr' + \int_r^\infty r'\rho_p(r')dr'\right], \tag{22}$$

where $Z_1 = 2$ in the case of α decay.

In the effective potential of Eq. (20), the isospin asymmetry effects are accounted for through the β and γ interaction terms. The parameter ϵ is introduced to account for the nuclear many-body effects in nuclei, but we found that the results are not sensitive to the value of ϵ, so we set $\epsilon = \frac{1}{6}$ throughout this study. The interaction parameters α, β, γ, δ, and η are fitted by minimizing the rms deviation. In this model, we also use the centrifugal barrier as given in Eq. (17), and this completes our model for the α nuclear potential based on the Skyrme EDF.

E. Empirical formula for α-decay half-lives with isospin effects

The Geiger-Nutall law gives a simple relationship of α-decay lifetimes to the proton number and the Q_α value [32]. The VS empirical formula, which is an improved form of the Geiger-Nutall law, is widely used to estimate the α-decay lifetimes, and it reads [33]

$$\log_{10}(T_{1/2}/\mathrm{s}) = \frac{aZ+b}{\sqrt{Q_\alpha/\mathrm{MeV}}} + cZ + d, \tag{23}$$

where a, b, c, and d are parameters to be fitted to the experimental data. In its original form, Eq. (23) contains an $h_{\log}$ term that takes into account the difference between the even and the odd nuclei. In this paper, we allow different values of the parameters for even or odd numbers of Z and N, so introducing the blocking factor for odd nucleus $h_{\log}$ is not necessary in our formula.

The subsequent efforts to improve this relation can be found, e.g., in Refs. [34–38]. Since the primary aim of the present paper is to look for the effects of nuclear isospin asymmetry, we simply modify the above formula as

$$\log_{10}(T_{1/2}/\mathrm{s}) = \frac{aZ+b}{\sqrt{Q_\alpha/\mathrm{MeV}}} + cZ + d + e_1I + e_2I^2, \tag{24}$$

where I is defined in Eq. (13).

III. RESULTS

In this section, we perform the fitting procedure described in Sec. II A and present the fitted parameters. We then compare our results with the available experimental data and give our predictions on the α-decay lifetimes of superheavy elements.

A. Fitted parameters

We begin with the simple SW potential model whose fitted parameters are presented in Tables I–III for four different

[4]As usual, it is understood that $\boldsymbol{k}'$ operates in the left bra space, whereas $\boldsymbol{k}$ operates in the right ket space.

TABLE I. Parameters of the SW potential fitted to the experimental data of Refs. [30,31]. The numbers in parentheses denote the fitted values without the V_1 and V_2 terms. The rms deviation σ is defined in Eq. (6).

Type	Number of events	V_0 (MeV)	V_1 (MeV)	V_2 (MeV)	σ
e-e	178	−140.035 (−132.415)	+57.567	−71.601	0.304 (0.319)
e-o	110	−175.980 (−140.416)	+524.995	−1737.533	0.596 (0.616)
o-e	137	−158.767 (−142.700)	+308.787	−1163.721	0.607 (0.630)
o-o	70	−152.100 (−144.250)	+56.482	−63.256	0.604 (0.609)

cases of α decays, namely, even-even (e-e), even-odd (e-o), odd-even (o-e), and odd-odd (o-o) where the former refers to the neutron number and the latter refers to the proton number of the decaying nucleus. For the fitting process, the AME2012 experimental data compiled in Refs. [30,31] are used. Numbers in parentheses denote the values obtained without the I and I^2 terms. Comparing the rms deviations σ for the cases with and without the isospin asymmetry terms, we notice a slight improvement due to the I and I^2 terms. The rms deviation σ value has the lowest value for the case of e-e nuclei and larger values for other nuclei. The main reason for this behavior is the assumed value ($\ell = 0$) of the orbital angular momentum. To verify this, we allow the variation of ℓ for each nuclei. It is then found that $\ell = 0$ gives a reasonable description of the decays of even-even nuclei, but $\ell \neq 0$ is definitely needed to have a better fit for the other nuclei. Since $\ell = 0$ is assumed for all nuclei in the SW potential model, there is a limit to reduce the σ values for even-odd, odd-even, and odd-odd nuclei. But we do not further pursue finding a better parameter set by varying the value of ℓ in this model as our purpose is to see the role of the isospin asymmetry terms compared with the model of Refs. [6,7].

Unlike the SW potential model discussed above, the $\ell = 0$ constraint is released in the WS potential model following the prescription of Ref. [8]. Tables IV–VI show the fitted parameters of the WS potential. We can see that the rms deviation in the case of even-even nuclei is similar in quality to that of the SW potential model. But the results for the other nuclei are improved a lot. The main reason is that, as was mentioned above, we allow the variation of ℓ in the fitting process. Namely, we change the ℓ value for each nucleus so that it reproduces the best result of rms deviation, whereas the condition of parity conservation is satisfied. As a result, we obtain a better result for the rms deviation. Inclusion of the isospin asymmetry term slightly improves the results of even-even nuclei but leaves the rms deviation almost unchanged for odd-N or odd-Z nuclei, which implies that, in this model, the angular momentum effect is much stronger than the isospin asymmetry effect.

Presented in Table VII are the parameters of the α nuclear potential from the Skyrme EDF. For the fitting process, we use the data only for even-even nuclei since the formula already includes the isospin dependence explicitly and the parameters should be the same for the four cases of the proton and neutron numbers. Table VII also displays the rms deviation values with the fitted parameters for four cases of nuclei. As in the WS potential model, we assume $\ell = 0$ for even-even nuclei but allow the change in ℓ for other nuclei, which results in smaller deviations for odd-N or odd-Z nuclei. The overall agreement with the measured data is as satisfactory as the WS potential model. More detailed comparison will be presented in the next subsection.

In order to see the model dependence of the results, we plot the obtained nuclear potentials of the α particle for the nucleus $^{294}_{118}$Uuo in Fig. 1. We find that the three models provide similar potentials but the structure of the potential in the inner region ($r < 10$ fm) shows rather strong model dependence. Namely, the WS potential gives the deepest potential, whereas the depths of SW and EDF potentials are similar to each other. Roughly speaking, the depth of the WS potential is bigger than those of the SW and EDF potentials by about 20%. On the other hand, the barrier width for a given value of Q_α takes the largest value for the WS potential and the smallest for the EDF one, but the difference is only less than 1 fm. Since the half-life is mostly determined by the quantum tunneling effects, the major factor that determines the lifetime is the potential width where the α particle should penetrate. Therefore, in the case of $^{294}_{118}$Uuo, we have the hierarchy of $T^{\rm SW}_{1/2} \simeq T^{\rm WS}_{1/2} > T^{\rm EDF}_{1/2}$ that is confirmed by numerical calculation.[5] This is so because a shorter penetration barrier gives a shorter lifetime. However, the inner part of the potential may affect the lifetime through the assaulting frequency $\mathcal{F}$ determined by the Q_α value. The results shown in Tables I–VII suggest that the isospin

[5]Of course, we have different relations among them depending on the nucleus.

TABLE II. Parameters of the SW potential fitted to the experimental data of Refs. [30,31]. The numbers in parentheses denote the fitted values without the V_1 term. The rms deviation σ is defined in Eq. (6).

Type	Number of events	V_0 (MeV)	V_1 (MeV)	σ
e-e	178	−138.523 (−132.415)	+35.644	0.304 (0.319)
e-o	110	−135.823 (−140.416)	+25.727	0.614 (0.616)
o-e	137	−134.579 (−142.700)	−46.412	0.620 (0.630)
o-o	70	−150.740 (−144.250)	+37.035	0.604 (0.609)

TABLE III. Parameters of the SW potential fitted to the experimental data of Refs. [30,31]. The numbers in parentheses denote the fitted values without the V_2 term. The rms deviation σ is defined in Eq. (6).

Type	Number of events	V_0 (MeV)	V_2 (MeV)	σ
e-e	178	−135.933 (−132.415)	+111.431	0.305 (0.319)
e-o	110	−136.899 (−140.416)	−105.036	0.612 (0.616)
o-e	137	−136.969 (−142.700)	−175.735	0.616 (0.630)
o-o	70	−148.022 (−144.250)	+116.513	0.604 (0.609)

asymmetry effects in SW and WS models are mostly involved in assaulting frequencies and the penetration lengths are almost unaffected. Therefore, the rms deviations are not improved much by the isospin asymmetry effect.

In the present paper, we also investigate the modified VS formula for the α-decay lifetimes. Tables VIII–X show our results on the fitted parameters for the modified VS formula and the corresponding rms deviation. The numbers in parentheses represent the results without the isospin asymmetric terms. Compared to the SW and WS potential models, inclusion of the isospin asymmetry term considerably improves the rms deviation. However, the obtained rms deviations are larger than the WS model, which may indicate some missed structure in the VS formula. First, in the (modified) VS formula, there is no room to incorporate the contribution of the angular momentum ℓ, i.e., the centrifugal barrier, so this may limit the application of the VS formula. Second, the α-decay lifetimes may have a more complicated dependence on isospin asymmetry other than the I and I^2 terms. Such effects could be accounted for through more realistic microscopic approaches.

B. Comparison with data

We present our results for α-decay half-lives of several heavy nuclei in Table XI, which shows the results from the SW potential model, the WS potential model, the Skyrme EDF potential model, and the VS formula, where the SW, WS, and VS models include the isospin asymmetry terms. The experimental Q_α values and measured half-lives of heavy nuclei are also given for comparison. The rms deviation σ given in this table is the value obtained with the listed 27 nuclei. All the models give half-lives consistent with the experimental data, and, at least, they are in the correct order of magnitude. Very few exceptional cases are the SW and VS models for the $(Z,A) = (111,279)$ nucleus and SW model for the cases of (107,270) and (109,274) where the theoretical values are smaller than the measured data by an order of magnitude. On the other hand, the Skyrme EDF model reproduces the experiment data fairly well, giving the ratio of theory to experiment in the range from 0.40 for (109,276) to 2.53 for (116,291).[6]

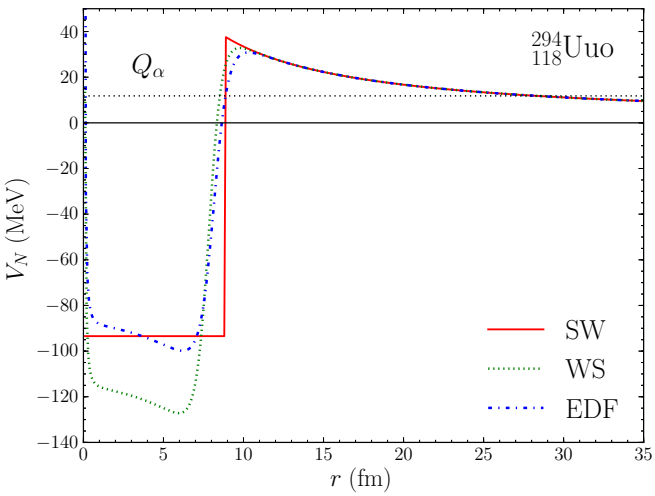

FIG. 1. The α-particle nuclear potential in the nucleus $^{294}_{118}$Uuo of the three models considered in the present paper.

Excellence of the EDF approach for the listed 27 heavy nuclei can be verified by the small value of the rms deviation as shown in the last row of Table XI. For the SW potential and the VS formula, the σ values are significantly larger than the values given in Tables I and IV that are obtained in the fitting. This may indicate the limitation of these models to describe α decays of heavy nuclei. As was mentioned earlier, the orbital angular momentum ℓ is set to be zero in the SW and VS models regardless of the type of decaying nuclei. On the other hand, this restriction is released for the WS and Skyrme EDF models, and consequently, they lead to better fittings. Nevertheless, it should be mentioned that the rms deviation value of the Skyrme EDF model in Table XI is even smaller than those in Table VII, and this indicates the usefulness of this model for describing α decays of heavy nuclei.

We also compare our results with those obtained in the unified fission model (UFM) of Ref. [43]. To this end we take Table I in Ref. [43] as a benchmark for our calcu-

[6]Our fitted parameters determined in this section without the isospin term are consistent with those of Refs. [6,7,37] for even-even nuclei considering the different sets of data used in the fitting procedure. In the present paper, for the SW and WS potentials, we carry out the fitting separately for even-even, even-odd, odd-even, and odd-odd nuclei.

TABLE IV. Fitted parameters of the WS potential. The notation is the same as in Table I.

Type	V_0 (MeV)	V_1 (MeV)	V_2 (MeV)	σ
e-e	−190.845 (−179.634)	+54.851	+56.370	0.302 (0.326)
e-o	−173.564 (−174.859)	+64.534	−38.600	0.211 (0.212)
o-e	−187.018 (−182.313)	+36.494	+127.714	0.248 (0.251)
o-o	−180.316 (−176.876)	−16.653	+86.544	0.254 (0.256)

TABLE V. Fitted parameters of the WS potential. The notation is the same as in Table I.

Type	V_0 (MeV)	V_1 (MeV)	σ
e-e	−191.785 (−179.634)	+70.737	0.302 (0.326)
e-o	−174.860 (−174.859)	−2.514	0.212 (0.212)
o-e	−182.293 (−182.313)	+0.965	0.251 (0.251)
o-o	−176.844 (−176.876)	−5.644	0.256 (0.256)

TABLE VI. Fitted parameters of the WS potential. The notation is the same as in Table I.

Type	V_0 (MeV)	V_2 (MeV)	σ
e-e	−182.314 (−179.634)	+90.277	0.311 (0.326)
e-o	−173.971 (−174.859)	−22.157	0.211 (0.212)
o-e	−184.537 (−182.313)	+61.693	0.249 (0.251)
o-o	−178.532 (−176.876)	+42.256	0.255 (0.256)

lation to have one-to-one comparison possible. For most nuclei the UFM also gives a good agreement with the experiment data except for several cases, such as $(Z,A) =$ (107,270), (109,274), (111,279), and (113, 282) where the UFM predictions are smaller than the measured data by a factor of 10 or more. On the other hand, the Skyrme EDF model of the present paper gives a quite reasonable description for these cases. The main reason is attributed to the fact that, in the Skyrme EDF model, the shape of the potential changes depending on the values of Z and A. By changing the values of Z and/or A, the parameters of the density profiles of the protons and neutrons in Eq. (21) need to be readjusted to find the minimum energy condition, which leads to the modification of the potential and thus the penetration length. Although the SW and WS potentials are somehow dependent on the neutron number through the quantization condition of Eq. (9),[7] the resulting half-lives indicate that the EDF model treats the modification of the potential in a more proper way. This again suggests that microscopic treatments of the nuclear potential are needed for more realistic approaches for understanding nuclear phenomena.

C. Predictions on undiscovered α-decay lifetimes of superheavy elements

The information on the α-decay lifetime can help experimentally confirm the synthesis of unknown superheavy elements. In this subsection we present our predictions on α decays of such elements. In this case, however, we do not have reliable information on the value of Q_α, so we have to rely on the predictions of theoretical models on nuclear structure. Since the α-decay lifetime is sensitive to the value of Q_α, this causes uncertainties in our estimates. In our calculation, we use the recent Weizsäcker-Skyrme4 (WS4) model of Ref. [44], which gives a good description for the nuclei of $Z \geqslant 100$. (See, for example, Refs. [45–47] for other models.) With nuclei masses the Q_α values can be calculated by [48]

$$Q_\alpha = \Delta M(Z,A) - \Delta M(Z-2,A-4) - \Delta M_\alpha + 10^{-6}k[Z^\beta - (Z-2)^\beta], \quad (25)$$

where ΔM is the atomic mass excess, $\Delta M_\alpha = 2.4249$ MeV, and $(k = 8.7$ eV, $\beta = 2.517)$ for nuclei of $Z \geqslant 60$ and $(k = 13.6$ eV, $\beta = 2.408)$ for nuclei of $Z < 60$.

[7]A part of the isospin asymmetry effects of α decay comes from the penetration length of the Coulomb potential which depends only on Z.

The obtained Q_α values for heavy nuclei of $Z = 117$–122 are listed in Table XII together with their α-decay half-lives predicted by the SW, WS, Skyrme EDF potential models, and the VS formula. Here, VS and VS0 denote the VS formula with and without the isospin asymmetry terms, respectively. The nuclei listed in Table XII are along the valley of small Q_α values. Because of the absence of the detailed information on their structures and quantum numbers, we simply assume $\ell = 0$. Graphs shown in Fig. 2 visualize the half-lives listed in Table XII. For a given value of Z, the α-decay lifetime actually depends on the Q_α value, and a longer lifetime is associated with a smaller Q_α value. Comparing the results of the VS and VS0 formulas, we can see that the inclusion of the isospin term increases lifetimes a little bit but does not make a significant difference.

Among the nuclei in Table XII, the lifetime of the (117,294) nucleus was reported very recently [49]. The reported experimental value of its lifetime is 54^{+94}_{-20} ms, which is about 20 times larger than our prediction of the Skyrme EDF model that gives 2.446 ms. We found that this discrepancy may be related to the difference of the Q_α value between the theoretical prediction and the measured value. The WS4 model predicts $Q_\alpha = 11.346$ MeV [44], but the measured value is 11.20 MeV [49]. The difference is only about 1.3%, but as can be seen in the Geiger-Nutall law or the VS formula of Eq. (23), the lifetime is very sensitive to the value of Q_α and a 1% difference in Q_α could result in a factor of 10 difference in the lifetime. This shows the sensitivity of the α-decay lifetime to the nuclear structure and the important role carried by Q_α in determination of nuclear half-lives.

In fact, if we use the measured Q_α value in our calculation, the obtained lifetimes are in good agreement with the measured lifetime as shown in Table XIII, which also summarizes the half-lives of the nuclei in the decay chain of the $^{294}117$ nucleus. In most cases the models we use in this paper reproduce the experimental data as good as in Table XI. However, we note that the theoretical predictions overestimate the lifetime of the (113,286) nucleus by one or two orders of magnitude, which

TABLE VII. Fitted parameters of the α-particle potential model based on the Skyrme EDF.

α (MeV fm^3)	β (MeV fm^5)	γ (MeV fm$^{6+3\epsilon}$)	δ (MeV fm^5)	η (MeV fm^5)
-1.6740×10^3	1.9208×10^3	1.7182×10^3	9.4166	−26.7616
σ(e-e)	σ(e-o)	σ(o-e)	σ(o-o)	σ(All)
0.319	0.276	0.283	0.301	0.296

TABLE VIII. Fitted coefficients of the modified VS formula. The values in parentheses are those of the unmodified VS formula, i.e., without the e_1 and e_2 terms.

Type	a	b	c	d	e_1	e_2	σ
e-e	1.53420 (1.48503)	4.20759 (5.26806)	−0.18124 (−0.18879)	−35.57934 (−33.89407)	5.28401	−38.17144	0.311 (0.359)
e-o	1.64322 (1.55427)	−2.33315 (1.23165)	−0.18749 (−0.18838)	−35.27841 (−34.29805)	1.19898	−31.24030	0.571 (0.608)
o-e	1.69868 (1.64654)	−5.67266 (−3.14939)	−0.22366 (−0.22053)	−32.02953 (−32.74153)	−12.96399	31.01813	0.542 (0.554)
o-o	1.37778 (1.34355)	13.63138 (13.92103)	−0.11009 (−0.12867)	−39.41075 (−37.19944)	5.98423	−52.56801	0.561 (0.617)

is similar to the observation mentioned in Ref. [50]. A more rigorous and complex analysis would be required to understand this discrepancy. At the bottom of Table XIII, therefore, we provide two sets of rms deviation values. The upper and lower rows represent the rms deviation values with and without the (113,286) nucleus, respectively. The advantage of including the isospin-dependent term is evident when we compare the results of the VS and VS0 formulas except the isotope of (113,286).

IV. CONCLUSION

The phenomenological potential for the α particle inside a nucleus and the WKB approximation are the two key concepts to investigate α-decay half-lives of nuclei in the cluster model. In the present paper, we propose to modify the nuclear potential of the α particle by explicitly including the isospin-dependent terms containing $I = (N - Z)/A$, and we calculated the α-decay half-lives of nuclei with the value of I as large as 0.2. We also suggest a new effective potential of the α particle based on the Skyrme energy density functional, which contains the isospin asymmetry contribution in a more natural way. Finally, we modified the empirical VS formula by including the I and I^2 terms.

Although the α-decay half-lives are mostly determined by the value of Q_α, we found that the isospin effects may improve the results to some extent as shown by our results. Together with the results of Ref. [16], which shows the importance of nuclear symmetry energy in Q_α values, our findings indicate the important role of nuclear isospin asymmetry effects in neutron-rich nuclei.

The potential model based on the Skyrme EDF suggests a form of the interaction between the α particle and the nucleon in the lowest order. The parameters of this approach are then obtained by fitting the α-decay half-lives. In addition, the density profile of the core nucleus was found by the Thomas-Fermi approximation. The proposed EDF approach for α decay was found to explain successfully the decay events of heavy nuclei even better than the square-well potential and Woods-Saxson potential approaches, which may be ascribed to the realistic density profile of the core nucleus based on a microscopic approach. This indicates that the isospin asymmetry may alter the penetration length of the potential barrier as well.

In the present paper, we first parametrize the nuclear potential of the α particle and fit the parameters to the data. Therefore, in this process, we cannot take into account the specific properties of each nucleus. As a result, the effects which come from, for example, the shell structure, deformation, and the preformation factor of the α particle could not be properly taken into account. Therefore, improving the present model calculations along this direction and inclusion of isospin asymmetry effects in microscopic models would be desired to better understand nuclear α decay of neutron-rich nuclei.

ACKNOWLEDGMENTS

We are grateful to N. Itagaki for fruitful discussions. This work was supported, in part, by the Basic Science Research Program through the National Research Foundation (NRF) of Korea funded by the Ministry of Education under Grants No. NRF-2013R1A1A2A10007294, No. NRF-2014R1A1A2054096, and No. NRF-2015R1D1A1A01059603. The work of Y.L. was supported by the Rare Isotope Science Project funded by the Ministry of Science, ICT and Future Planning (MSIP) of the Korean Government and the National Research Foundation (NRF) of Korea under Grant No. 2013M7A1A1075766.

APPENDIX

In microscopic approaches, the α-particle bound state with a nucleus can be studied by solving the Hartree-Fock equation. As given in Eq. (18), we start with the potential in the

TABLE IX. Fitted coefficients of the modified VS formula. The values in parentheses are those of the unmodified VS formula, i.e., without the e_1 term.

Type	a	b	c	d	e_1	σ
e-e	1.53223 (1.48503)	4.33481 (5.26806)	−0.18002 (−0.18879)	−34.97023 (−33.89407)	−5.77017	0.327 (0.359)
e-o	1.62853 (1.55427)	−1.43833 (1.23165)	−0.18372 (−0.18838)	−34.83250 (−34.29805)	−8.12715	0.573 (0.608)
o-e	1.68262 (1.64654)	−4.30929 (−3.14939)	−0.21807 (−0.22053)	−33.11939 (−32.74153)	−3.73747	0.547 (0.554)
o-o	1.43614 (1.34355)	10.05247 (13.92103)	−0.12664 (−0.12867)	−37.45332 (−37.19944)	−9.64627	0.570 (0.617)

TABLE X. Fitted coefficients of the modified VS formula. The values in parentheses are those of the unmodified VS formula, i.e., without the e_2 terms.

Type	a	b	c	d	e_2	σ
e-e	1.53829 (1.48503)	4.16407 (5.26806)	−0.17981 (−0.18879)	−35.39178 (−33.89407)	−22.00448	0.314 (0.359)
e-o	1.64186 (1.55427)	−2.23887 (1.23165)	−0.18700 (−0.18838)	−35.22664 (−34.29805)	−27.38784	0.571 (0.608)
o-e	1.66663 (1.64654)	−3.56210 (−3.14939)	−0.21732 (−0.22053)	−33.29803 (−32.74153)	−8.53409	0.550 (0.554)
o-o	1.40242 (1.34355)	12.19381 (13.92103)	−0.11593 (−0.12867)	−38.72067 (−37.19944)	−33.75875	0.563 (0.617)

form of

$$\begin{aligned} v_{N\alpha}(\boldsymbol{k},\boldsymbol{k}') = {} & s_0(1+v_0P_\sigma)\delta(\boldsymbol{r}_{N\alpha}) \\ & + \frac{s_1}{2}(1+v_1P_\sigma)[\delta(\boldsymbol{r}_{N\alpha})\boldsymbol{k}^2 + \boldsymbol{k}'^2\delta(\boldsymbol{r}_{N\alpha})] \\ & + s_2\boldsymbol{k}'\cdot\delta(\boldsymbol{r}_{N\alpha})\boldsymbol{k} + iW_0^\alpha\boldsymbol{k}'\cdot(\boldsymbol{\sigma}\times\boldsymbol{k})\delta(\boldsymbol{r}_{N\alpha}) \\ & + \frac{s_3}{6}(1+v_3P_\sigma)\rho_N^\epsilon\delta(\boldsymbol{r}_{N\alpha}). \end{aligned} \tag{A1}$$

When kinetic energy is included, the above interaction leads to the Hamiltonian for the α particle as

$$\begin{aligned} \mathcal{H}_\alpha = {} & \frac{\hbar^2}{2m_\alpha}\tau_\alpha + s_0\left(1+\frac{v_0}{2}\right)\rho_N\rho_\alpha + \frac{1}{4}(s_1+s_2)(\tau_\alpha\rho_N+\tau_N\rho_\alpha) \\ & + \frac{1}{4}(3s_1-s_2)(\boldsymbol{\nabla}\rho_N\cdot\boldsymbol{\nabla}\rho_\alpha) \end{aligned}$$

TABLE XI. Results for α-decay half-lives of heavy nuclei. The upper and lower bounds of theoretical calculations are from the experimental errors of Q_α values.

(Z,A)	$Q_\alpha^{\text{Expt.}}$ (MeV)	$T_{1/2}^{\text{Expt.}}$	$T_{1/2}^{\text{SW}}$	$T_{1/2}^{\text{WS}}$	$T_{1/2}^{\text{EDF}}$	$T_{1/2}^{\text{VS}}$	References
(118,294)	11.81 ± 0.06	$0.89^{+1.07}_{-0.31}$ ms	$1.46^{+0.51}_{-0.38}$ ms	$1.26^{+0.45}_{-0.33}$ ms	$0.40^{+0.15}_{-0.11}$ ms	$0.31^{+0.12}_{-0.08}$ ms	[39]
(116,293)	10.67 ± 0.06	53^{+62}_{-19} ms	163^{+69}_{-48} ms	104^{+44}_{-31} ms	52^{+23}_{-16} ms	181^{+84}_{-57} ms	[40]
(116,292)	10.80 ± 0.07	18^{+16}_{-6} ms	78^{+39}_{-26} ms	69^{+35}_{-23} ms	25^{+13}_{-8} ms	20^{+10}_{-7} ms	[40]
(116,291)	10.89 ± 0.07	$6.3^{+11.6}_{-2.5}$ ms	47^{+23}_{-15} ms	31^{+15}_{-10} ms	16^{+8}_{-5} ms	46^{+25}_{-16} ms	[39]
(116,290)	11.00 ± 0.08	$7.1^{+3.2}_{-1.7}$ ms	$25.9^{+14.5}_{-9.2}$ ms	$23.2^{+13.2}_{-8.3}$ ms	$8.9^{+5.0}_{-3.3}$ ms	$7.2^{+4.2}_{-2.6}$ ms	[39]
(115,288)	10.61 ± 0.06	87^{+105}_{-30} ms	115^{+48}_{-34} ms	139^{+60}_{-41} ms	43^{+19}_{-13} ms	676^{+279}_{-196} ms	[41]
(115,287)	10.74 ± 0.09	32^{+155}_{-14} ms	55^{+37}_{-22} ms	50^{+34}_{-20} ms	21^{+15}_{-8} ms	131^{+97}_{-55} ms	[41]
(114,289)	9.96 ± 0.06	$2.7^{+1.4}_{-0.7}$ s	$2.8^{+1.3}_{-0.9}$ s	$3.1^{+1.5}_{-1.0}$ s	$1.1^{+0.5}_{-0.3}$ s	$4.8^{+2.5}_{-1.6}$ s	[40]
(114,288)	10.09 ± 0.07	$0.8^{+0.32}_{-0.18}$ s	$1.2^{+0.68}_{-0.43}$ s	$1.12^{+0.63}_{-0.40}$ s	$0.48^{+0.27}_{-0.17}$ s	$0.39^{+0.22}_{-0.14}$ s	[40]
(114,287)	10.16 ± 0.06	$0.48^{+0.16}_{-0.09}$ s	$0.80^{+0.36}_{-0.25}$ s	$0.53^{+0.24}_{-0.17}$ s	$0.32^{+0.15}_{-0.10}$ s	$1.23^{+0.61}_{-0.41}$ s	[39]
(114,286)	10.33 ± 0.06	$0.13^{+0.04}_{-0.02}$ s	$0.29^{+0.13}_{-0.09}$ s	$0.26^{+0.12}_{-0.08}$ s	$0.12^{+0.05}_{-0.04}$ s	$0.10^{+0.04}_{-0.03}$ s	[39]
(113,284)	10.15 ± 0.06	$0.48^{+0.58}_{-0.17}$ s	$0.40^{+0.18}_{-0.12}$ s	$0.50^{+0.23}_{-0.16}$ s	$0.28^{+0.13}_{-0.09}$ s	$2.12^{+0.93}_{-0.64}$ s	[41]
(113,283)	10.26 ± 0.09	100^{+490}_{-45} ms	209^{+152}_{-87} ms	62^{+45}_{-26} ms	91^{+69}_{-39} ms	563^{+445}_{-246} ms	[41]
(113,282)	10.83 ± 0.08	73^{+134}_{-29} ms	8^{+4}_{-3} ms	52^{+30}_{-19} ms	75^{+44}_{-28} ms	52^{+29}_{-18} ms	[42]
(112,285)	9.29 ± 0.06	34^{+17}_{-9} s	50^{+27}_{-17} s	34^{+18}_{-12} s	23^{+12}_{-8} s	133^{+76}_{-48} s	[40]
(112,283)	9.67 ± 0.06	$3.8^{+1.2}_{-0.7}$ s	$3.9^{+1.9}_{-1.3}$ s	$4.5^{+2.2}_{-1.5}$ s	$1.8^{+0.9}_{-0.6}$ s	$8.4^{+4.4}_{-2.9}$ s	[39]
(111,280)	9.87 ± 0.06	$3.6^{+4.3}_{-1.3}$ s	$0.50^{+0.23}_{-0.16}$ s	$3.7^{+1.7}_{-1.2}$ s	$6.0^{+2.9}_{-1.9}$ s	$2.4^{+1.1}_{-0.7}$ s	[41]
(111,279)	10.52 ± 0.16	170^{+810}_{-80} ms	10^{+16}_{-6} ms	62^{+96}_{-37} ms	110^{+177}_{-67} ms	23^{+39}_{-14} ms	[41]
(111,278)	10.89 ± 0.08	$4.2^{+7.5}_{-1.7}$ ms	$1.4^{+0.7}_{-0.5}$ ms	$2.7^{+1.5}_{-0.9}$ ms	$2.7^{+1.6}_{-1.0}$ ms	$8.2^{+4.4}_{-2.9}$ ms	[42]
(110,279)	9.84 ± 0.06	$0.20^{+0.05}_{-0.04}$ s	$0.28^{+0.13}_{-0.09}$ s	$0.18^{+0.08}_{-0.06}$ s	$0.13^{+0.06}_{-0.04}$ s	$0.59^{+0.30}_{-0.20}$ s	[39]
(109,276)	9.85 ± 0.06	$0.72^{+0.97}_{-0.25}$ s	$0.12^{+0.05}_{-0.04}$ s	$0.88^{+0.41}_{-0.28}$ s	$0.29^{+0.14}_{-0.09}$ s	$0.52^{+0.23}_{-0.16}$ s	[41]
(109,275)	10.48 ± 0.09	$9.7^{+46}_{-4.4}$ ms	$3.0^{+2.0}_{-1.2}$ ms	$18.6^{+12.5}_{-7.4}$ ms	$6.7^{+4.6}_{-2.7}$ ms	$6.3^{+4.5}_{-2.6}$ ms	[41]
(109,274)	9.95 ± 0.10	440^{+810}_{-170} ms	67^{+56}_{-30} ms	480^{+416}_{-220} ms	172^{+153}_{-80} ms	353^{+294}_{-159} ms	[42]
(108,275)	9.44 ± 0.06	$0.19^{+0.22}_{-0.07}$ s	$0.75^{+0.36}_{-0.24}$ s	$0.48^{+0.24}_{-0.16}$ s	$0.39^{+0.20}_{-0.13}$ s	$2.12^{+1.12}_{-0.73}$ s	[39]
(107,272)	9.15 ± 0.06	$9.8^{+11.7}_{-3.5}$ s	$2.3^{+1.2}_{-0.8}$ s	$5.3^{+2.8}_{-1.8}$ s	$7.0^{+3.7}_{-2.4}$ s	$8.7^{+4.3}_{-2.9}$ s	[41]
(107,270)	9.11 ± 0.08	61^{+292}_{-28} s	$3.1^{+2.3}_{-1.3}$ s	25^{+19}_{-11} s	60^{+46}_{-26} s	14^{+10}_{-6} s	[42]
(106,271)	8.67 ± 0.08	$1.9^{+2.4}_{-0.6}$ min	$0.51^{+0.41}_{-0.22}$ min	$2.06^{+1.71}_{-0.92}$ min	$1.67^{+1.41}_{-0.76}$ min	$2.28^{+2.01}_{-1.06}$ min	[39]
σ			0.616	0.290	0.238	0.513	

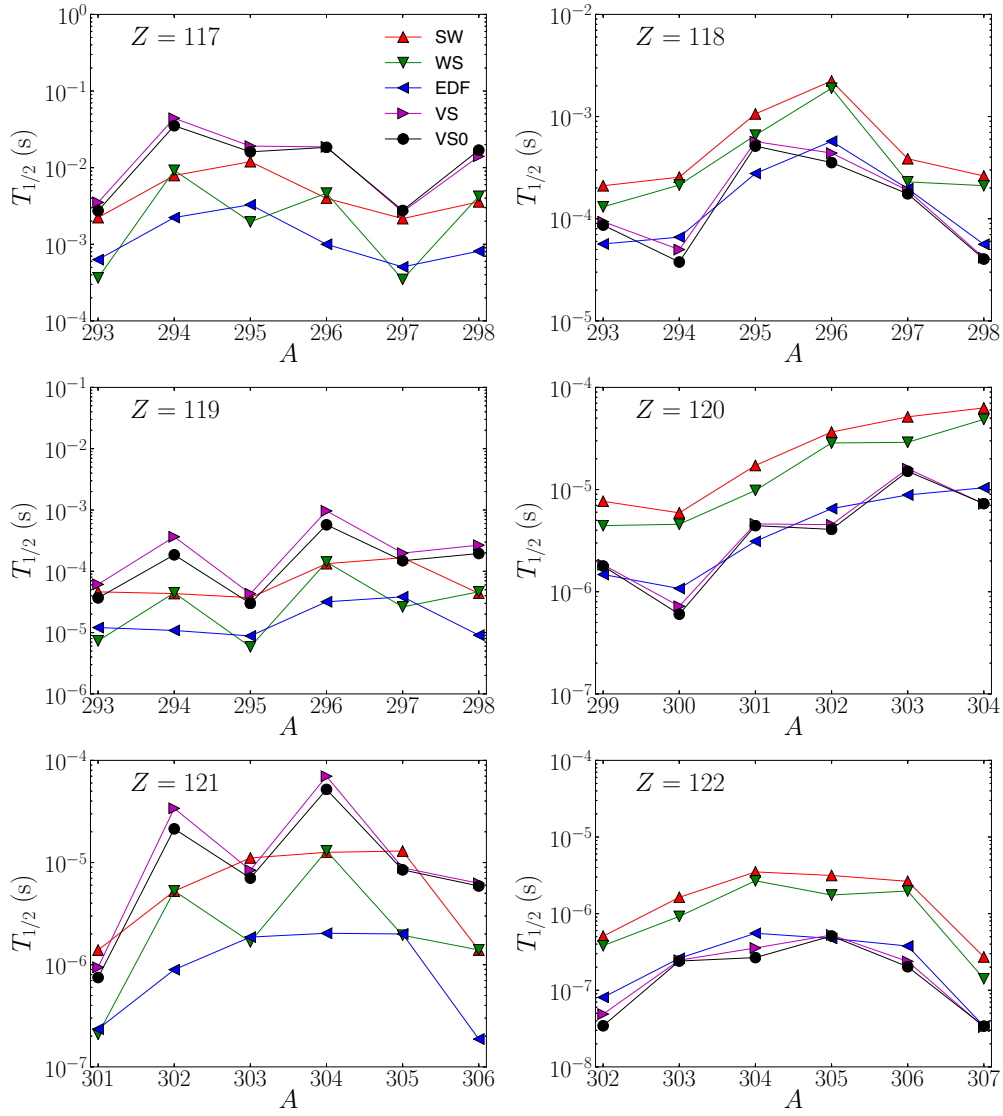

FIG. 2. Half-lives of superheavy elements listed in Table XII. The horizontal axis denotes the atomic mass number, and the vertical axis represents the half-life in units of seconds.

$$+\frac{1}{4}s_3\rho_N^{\epsilon}\rho_\alpha(\rho_N^2+2\rho_n\rho_p)$$
$$+\frac{1}{2}W_0^\alpha(\nabla\rho_N\cdot\boldsymbol{J}_\alpha+\nabla\rho_\alpha\cdot\boldsymbol{J}_N), \tag{A2}$$

where τ and $\boldsymbol{J}$ are expressed as

$$\tau_A(\boldsymbol{r})=\sum_i|\nabla\varphi_i|^2,\qquad \boldsymbol{J}_A(\boldsymbol{r})=\sum_i\varphi_i^\dagger(-i\nabla\times\boldsymbol{\sigma})\varphi_i \tag{A3}$$

for the nucleon ($A=N$) and the α particle ($A=\alpha$). The single-particle wave-function $\varphi(\boldsymbol{r})$ of the α particle can be obtained by solving the Hartree-Fock equation. In the spherically symmetric case, the wave function can be written as

$$\varphi_i(\boldsymbol{r})=\frac{R_{n\ell j}(r)}{r}\langle\ell m_\ell s\sigma|jm\rangle\,Y_m^\ell(\hat{\boldsymbol{r}}), \tag{A4}$$

and the Schrödinger equation becomes

$$\left[-\frac{d}{dr}\frac{\hbar^2}{2m_\alpha^*}\frac{d}{dr}+\frac{\hbar^2}{2m_\alpha^*}\frac{\ell(\ell+1)}{r^2}+V_N(r)\right]R_{n\ell j}(r)$$
$$=e_{n\ell j}R_{n\ell j}(r), \tag{A5}$$

where the potential for the α particle reads

$$V_N(\boldsymbol{r})=s_0\left(1+\frac{1}{2}v_0\right)\rho_N+\frac{1}{4}(s_1+s_2)(\tau_p+\tau_n)$$
$$-\frac{1}{4}(3s_1-s_2)\rho_N''-\left(\frac{5}{4}s_1-\frac{3}{4}s_2\right)\frac{\rho_N'}{r}$$
$$+\frac{1}{4}s_3\rho_N^{\epsilon}\left(\rho_N^2+2\rho_n\rho_p\right)-\frac{W_0^\alpha}{2}\left(J_N'+\frac{2}{r}J_N\right)$$
$$+\frac{1}{2}W_0^\alpha\frac{\rho_N'}{r}\left[j(j+1)-\ell(\ell+1)-\frac{3}{4}\right], \tag{A6}$$

TABLE XII. Theoretical predictions on α-decay lifetimes of superheavy elements. The Q_α values are calculated with the WS4 mass table [44]. The modified and unmodified Viola-Seaborg formulas are represented by VS and VS0, respectively.

Nuclei (Z,A)	Q_α (MeV)	$T_{1/2}^{\mathrm{SW}}$ (s)	$T_{1/2}^{\mathrm{WS}}$ (s)	$T_{1/2}^{\mathrm{EDF}}$ (s)	$T_{1/2}^{\mathrm{VS}}$ (s)	$T_{1/2}^{\mathrm{VS0}}$ (s)
(122,307)	14.360	2.721×10^{-7}	1.417×10^{-7}	3.401×10^{-8}	3.315×10^{-8}	3.402×10^{-8}
(122,306)	13.775	2.641×10^{-6}	1.975×10^{-6}	3.777×10^{-7}	2.380×10^{-7}	2.026×10^{-7}
(122,305)	13.734	3.147×10^{-6}	1.749×10^{-6}	4.746×10^{-7}	5.266×10^{-7}	5.103×10^{-7}
(122,304)	13.710	3.503×10^{-6}	2.684×10^{-6}	5.544×10^{-7}	3.563×10^{-7}	2.669×10^{-7}
(122,303)	13.904	1.630×10^{-6}	9.198×10^{-7}	2.614×10^{-7}	2.468×10^{-7}	2.405×10^{-7}
(122,302)	14.208	5.069×10^{-7}	3.820×10^{-7}	8.078×10^{-8}	4.887×10^{-8}	3.438×10^{-8}
(121,306)	13.783	1.392×10^{-6}	1.396×10^{-6}	1.873×10^{-7}	6.268×10^{-6}	5.896×10^{-6}
(121,305)	13.242	1.296×10^{-5}	1.943×10^{-6}	1.999×10^{-6}	8.881×10^{-6}	8.478×10^{-6}
(121,304)	13.251	1.259×10^{-5}	1.302×10^{-5}	2.030×10^{-6}	6.994×10^{-5}	5.196×10^{-5}
(121,303)	13.283	1.109×10^{-5}	1.673×10^{-6}	1.864×10^{-6}	8.416×10^{-6}	7.039×10^{-6}
(121,302)	13.464	5.247×10^{-6}	5.273×10^{-6}	8.943×10^{-7}	3.391×10^{-5}	2.137×10^{-5}
(121,301)	13.795	1.391×10^{-6}	2.086×10^{-7}	2.344×10^{-7}	9.437×10^{-7}	7.494×10^{-7}
(120,304)	12.736	6.297×10^{-5}	4.862×10^{-5}	1.041×10^{-5}	7.245×10^{-6}	7.286×10^{-6}
(120,303)	12.782	5.151×10^{-5}	2.901×10^{-5}	8.859×10^{-6}	1.602×10^{-5}	1.509×10^{-5}
(120,302)	12.862	3.656×10^{-5}	2.857×10^{-5}	6.506×10^{-6}	4.532×10^{-6}	4.074×10^{-6}
(120,301)	13.036	1.721×10^{-5}	9.805×10^{-6}	3.117×10^{-6}	4.612×10^{-6}	4.434×10^{-6}
(120,300)	13.290	5.916×10^{-6}	4.575×10^{-6}	1.075×10^{-6}	7.214×10^{-7}	6.024×10^{-7}
(120,299)	13.230	7.675×10^{-6}	4.437×10^{-6}	1.475×10^{-6}	1.836×10^{-6}	1.784×10^{-6}
(119,298)	12.684	4.371×10^{-5}	4.629×10^{-5}	9.081×10^{-6}	2.667×10^{-4}	1.950×10^{-4}
(119,297)	12.394	1.663×10^{-4}	2.624×10^{-5}	3.829×10^{-5}	1.981×10^{-4}	1.486×10^{-4}
(119,296)	12.444	1.331×10^{-4}	1.419×10^{-4}	3.180×10^{-5}	9.659×10^{-4}	5.733×10^{-4}
(119,295)	12.727	3.716×10^{-5}	5.852×10^{-6}	8.815×10^{-6}	4.307×10^{-5}	2.988×10^{-5}
(119,294)	12.695	4.332×10^{-5}	4.460×10^{-5}	1.084×10^{-5}	3.657×10^{-4}	1.857×10^{-4}
(119,293)	12.683	4.620×10^{-5}	7.336×10^{-6}	1.208×10^{-5}	6.122×10^{-5}	3.680×10^{-5}
(118,298)	12.153	2.621×10^{-4}	2.108×10^{-4}	5.623×10^{-5}	4.151×10^{-5}	4.030×10^{-5}
(118,297)	12.074	3.867×10^{-4}	2.296×10^{-4}	1.967×10^{-4}	1.893×10^{-4}	1.754×10^{-4}
(118,296)	11.722	2.232×10^{-3}	1.894×10^{-3}	5.727×10^{-4}	4.395×10^{-4}	3.546×10^{-4}
(118,295)	11.872	1.062×10^{-3}	6.571×10^{-4}	2.772×10^{-4}	5.688×10^{-4}	5.141×10^{-4}
(118,294)	12.167	2.553×10^{-4}	2.138×10^{-4}	6.608×10^{-5}	4.991×10^{-5}	3.770×10^{-5}
(118,293)	12.210	2.103×10^{-4}	1.307×10^{-4}	5.665×10^{-5}	9.354×10^{-5}	8.666×10^{-5}
(117,298)	11.490	3.580×10^{-3}	4.226×10^{-3}	8.133×10^{-4}	1.405×10^{-2}	1.693×10^{-2}
(117,297)	11.589	2.162×10^{-3}	3.478×10^{-4}	5.065×10^{-4}	2.652×10^{-3}	2.762×10^{-3}
(117,296)	11.473	3.972×10^{-3}	4.647×10^{-3}	9.994×10^{-4}	1.868×10^{-2}	1.840×10^{-2}
(117,295)	11.266	1.197×10^{-2}	1.960×10^{-3}	3.285×10^{-3}	1.911×10^{-2}	1.610×10^{-2}
(117,294)	11.346	7.897×10^{-3}	9.230×10^{-3}	2.232×10^{-3}	4.413×10^{-2}	3.526×10^{-2}
(117,293)	11.591	2.228×10^{-3}	3.643×10^{-4}	6.314×10^{-4}	3.518×10^{-3}	2.741×10^{-3}

TABLE XIII. Half-lives of nuclides in the decay chain of the nucleus $^{294}117$. The experimental data are from Ref. [49].

(Z,A)	Q_α (MeV)	$T_{1/2}^{\mathrm{Expt.}}$	$T_{1/2}^{\mathrm{SW}}$	$T_{1/2}^{\mathrm{WS}}$	$T_{1/2}^{\mathrm{EDF}}$	$T_{1/2}^{\mathrm{VS}}$	$T_{1/2}^{\mathrm{VS0}}$
(117,294)	11.20 $\pm$ 0.04	51^{+94}_{-20} ms	17^{+4}_{-3} ms	34^{+9}_{-7} ms	22^{+6}_{-4} ms	96^{+23}_{-18} ms	75^{+18}_{-14} ms
(115,290)	10.45 $\pm$ 0.04	$1.3^{+2.3}_{-0.5}$ s	$0.29^{+0.08}_{-0.06}$ s	$2.0^{+0.56}_{-0.44}$ s	$2.3^{+0.64}_{-0.50}$ s	$1.40^{+0.37}_{-0.29}$ s	$1.28^{+0.33}_{-0.26}$ s
(113,286)	9.4 $\pm$ 0.3	$2.9^{+5.3}_{-1.1}$ s	53^{+398}_{-46} s	71^{+552}_{-62} s	24^{+191}_{-21} s	208^{+1452}_{-179} s	209^{+1390}_{-179} s
(111,282)	9.18 $\pm$ 0.03	$3.1^{+5.7}_{-1.2}$ min	$0.81^{+0.19}_{-0.16}$ min	$1.91^{+0.46}_{-0.37}$ min	$1.96^{+0.48}_{-0.38}$ min	$2.88^{+0.66}_{-0.54}$ min	$3.60^{+0.81}_{-0.66}$ min
(109,278)	9.59 $\pm$ 0.03	$3.6^{+6.5}_{-1.4}$ s	$0.61^{+0.13}_{-0.11}$ s	$4.70^{+1.03}_{-0.84}$ s	$1.44^{+0.32}_{-0.26}$ s	$2.13^{+0.45}_{-0.37}$ s	$3.63^{+0.75}_{-0.62}$ s
(107,274)	8.97 $\pm$ 0.03	30^{+54}_{-12} s	$8.0^{+1.9}_{-1.5}$ s	$18.8^{+4.5}_{-3.6}$ s	$22.9^{+5.6}_{-4.5}$ s	$23.6^{+5.5}_{-4.4}$ s	$48.0^{+10.8}_{-8.8}$ s
(105,270)	8.02 $\pm$ 0.03	$1.0^{+1.9}_{-0.4}$ h	$0.57^{+0.16}_{-0.12}$ h	$0.82^{+0.23}_{-0.18}$ h	$0.39^{+0.11}_{-0.09}$ h	$1.27^{+0.35}_{-0.27}$ h	$2.91^{+0.78}_{-0.61}$ h
σ			0.769	0.592	0.486	0.773	0.790
			0.625	0.185	0.340	0.173	0.241

where $\rho_N = \rho_p + \rho_n$ with $\rho'_N = d\rho_N/dr$ and $\rho''_N = d^2\rho_N/dr^2$. The effective mass m^*_α is defined by

$$\frac{\hbar^2}{2m^*_\alpha} = \frac{\hbar^2}{2m_\alpha} + \frac{1}{4}(s_1 + s_2)\rho_N. \tag{A7}$$

Since the total spin of the α particle is zero, i.e., $\langle\sigma_\alpha\rangle = 0$, the spin-orbit coupling between the α particle and the daughter nucleus may be neglected. This process leads to the form of the effective potential of the α particle as

$$V_N = \alpha\rho_N + \beta\left(\rho_n^{5/3} + \rho_p^{5/3}\right) + \gamma\rho_N^{\epsilon}\left(\rho_N^2 + 2\rho_n\rho_p\right) + \delta\frac{\rho'_N}{r} + \eta\rho''_N, \tag{A8}$$

where we have used that $\tau_{p,n} \simeq \frac{3}{5}(3\pi^2)^{2/3}\rho_{p,n}^{5/3}$ within the Thomas-Fermi approximation.

[1] H. J. Mang, Alpha decay, Annu. Rev. Nucl. Sci. **14**, 1 (1964).
[2] Facility for Antiproton and Ion Research in Europe GmbH, http://www.fair-center.eu.
[3] FRIB Users Organization, http://fribusers.org/frib/science.html.
[4] S. Hofmann and G. Munzenberg, The discovery of the heaviest elements, Rev. Mod. Phys. **72**, 733 (2000).
[5] B.-A. Li, L.-W. Chen, and C. M. Ko, Recent progress and new challenges in isospin physics with heavy-ion reactions, Phys. Rep. **464**, 113 (2008).
[6] B. Buck, A. C. Merchant, and S. M. Perez, Ground state to ground state alpha decays of heavy even-even nuclei, J. Phys. G **17**, 1223 (1991).
[7] B. Buck, A. C. Merchant, and S. M. Perez, Favoured alpha decays of odd-mass nuclei, J. Phys. G **18**, 143 (1992).
[8] B. Buck, A. C. Merchant, and S. M. Perez, α decay calculations with a realistic potential, Phys. Rev. C **45**, 2247 (1992).
[9] G. Royer, Alpha emission and spontaneous fission through quasi-molecular shapes, J. Phys. G **26**, 1149 (2000).
[10] J. Dong, H. Zhang, Y. Wang, W. Zuo, and J. Li, Alpha-decay for heavy nuclei in the ground and isomeric states, Nucl. Phys. A **832**, 198 (2010).
[11] P. Roy Chowdhury, C. Samanta, and D. N. Basu, α decay half-lives of new superheavy elements, Phys. Rev. C **73**, 014612 (2006).
[12] C. Samanta, P. R. Chowdhury, and D. N. Basu, Predictions of alpha decay half lives of heavy and superheavy elements, Nucl. Phys. A **789**, 142 (2007).
[13] P. Roy Chowdhury, C. Samanta, and D. N. Basu, Search for long lived heaviest nuclei beyond the valley of stability, Phys. Rev. C **77**, 044603 (2008).
[14] V. Y. Denisov and H. Ikezoe, α-nucleus potential for α-decay and sub-barrier fusion, Phys. Rev. C **72**, 064613 (2005).
[15] L.-L. Li, S.-G. Zhou, E.-G. Zhao, and W. Scheid, A new barrier penetration formula and its application to alpha-decay half-lives, Int. J. Mod. Phys. E **19**, 359 (2010).
[16] J. Dong, W. Zuo, and W. Schied, Correlation Between α-Decay Energies of Superheavy Nuclei Involving the Effects of Symmetry Energy, Phys. Rev. Lett. **107**, 012501 (2011).
[17] J. Dong, W. Zuo, and J. Gu, Origin of symmetry energy in finite nuclei and density dependence of nuclear matter symmetry energy from measured α-decay energies, Phys. Rev. C **87**, 014303 (2013).
[18] C.-Y. Ryu, C. H. Hyun, and C.-H. Lee, Hyperons and nuclear symmetry energy in neutron star matter, Phys. Rev. C **84**, 035809 (2011).
[19] S. Gandolfi, J. Carlson, and S. Reddy, Maximum mass and radius of neutron stars, and the nuclear symmetry energy, Phys. Rev. C **85**, 032801(R) (2012).
[20] M. B. Tsang *et al.*, Constraints on the symmetry energy and neutron skins from experiments and theory, Phys. Rev. C **86**, 015803 (2012).
[21] J. M. Lattimer and Y. Lim, Constraining the symmetry parameters of the nuclear interaction, Astrophys. J. **771**, 51 (2013).
[22] C. Drischler, V. Somà, and A. Schwenk, Microscopic calculations and energy expansions for neutron-rich matter, Phys. Rev. C **89**, 025806 (2014).
[23] S. A. Gurvitz and G. Kalbermann, The Decay Width and the Shift of a Quasistationary State, Phys. Rev. Lett. **59**, 262 (1987).
[24] S. Åberg, P. B. Semmes, and W. Nazarewicz, Spherical proton emitters, Phys. Rev. C **56**, 1762 (1997); **58**, 3011(E) (1998).
[25] R. D. Woods and D. S. Saxon, Diffuse surface optical model for nucleon-nuclei scattering, Phys. Rev. **95**, 577 (1954).
[26] R. L. Varner, W. J. Thompson, T. L. McAbee, E. J. Ludwig, and T. B. Clegg, A global nucleon optical model potential, Phys. Rep. **201**, 57 (1991).
[27] E. Chabanat, P. Bonche, P. Haensel, J. Meyer, and R. Schaeffer, A Skyrme parametrization from subnuclear to neutron star densities Part II. Nuclei far from stabilities, Nucl. Phys. A **635**, 231 (1998).
[28] R. E. Langer, On the connection formulas and the solutions of the wave equation, Phys. Rev. **51**, 669 (1937).
[29] D. Vautherin and D. M. Brink, Hartree-Fock calculations with Skyrme's interaction. I. Spherical nuclei, Phys. Rev. C **5**, 626 (1972).
[30] G. Audi, M. Wang, A. H. Wapstra, F. G. Kondev, M. MacCormick, X. Xu, and B. Pfeiffer, The AME2012 atomic mass evaluation (I). Evaluation of input data, adjustment procedures, Chin. Phys. C **36**, 1287 (2012).
[31] M. Wang, G. Audi, A. H. Wapstra, F. G. Kondev, M. MacCormick, X. Xu, and B. Pfeiffer, The AME2012 atomic mass evaluation (II). Tables, graphs and references, Chin. Phys. C **36**, 1603 (2012).
[32] H. Geiger and J. M. Nuttall, The ranges of the α particles from various substances and a relation between range and period of transformation, Philos. Mag. Ser. 6 **22**, 613 (1911).
[33] V. E. Viola, Jr. and G. T. Seaborg, Nuclear systematics of the heavy elements - II. Lifetimes for alpha, beta and spontaneous fission decay, J. Inorg. Nucl. Chem. **28**, 741 (1966).
[34] Z. Ren, C. Xu, and Z. Wang, New perspective on complex cluster radioactivity of heavy nuclei, Phys. Rev. C **70**, 034304 (2004).
[35] G. Royer and H. F. Zhang, Recent α decay half-lives and analytic expression predictions including superheavy nuclei, Phys. Rev. C **77**, 037602 (2008).

[36] D. Ni, Z. Ren, T. Dong, and C. Xu, Unified formula of half-lives for α decay and cluster radioactivity, Phys. Rev. C **78**, 044310 (2008).

[37] A. Sobiczewski, Z. Patyk, and S. Ćwiok, Deformed superheavy nuclei, Phys. Lett. B **224**, 1 (1989).

[38] K. P. Santhosh, I. Sukumaran, and B. Priyanka, Theoretical studies on the alphs decay of $^{178-220}$Pb isotopes, Nucl. Phys. A **935**, 28 (2015).

[39] Yu. Ts. Oganessian *et al.*, Synthesis of the isotopes of elements 118 and 116 in the ^{249}Cf and ^{249}Cm + ^{48}Ca fusion reactions, Phys. Rev. C **74**, 044602 (2006).

[40] Yu. Ts. Oganessian *et al.*, Measurements of cross sections and decay properties of the isotopes of elements 112, 114, and 116 produced in the fusion reactions ^{233,238}U, ^{242}Pu, and ^{248}Cm + ^{48}Ca, Phys. Rev. C **70**, 064609 (2004); **71**, 029902(E) (2005).

[41] Yu. Ts. Oganessian *et al.*, Experiments on the synthesis of element 115 in the reaction ^{243}Am(^{48}Ca ,xn)$^{291-x}$115, Phys. Rev. C **69**, 021601(R) (2004); **69**, 029902(E) (2004); Synthesis of elements 115 and 113 in the reaction ^{243}Am + ^{48}Ca, **72**, 034611 (2005).

[42] Yu. Ts. Oganessian *et al.*, Synthesis of the isotope ^{282}113 in the ^{237}Np + ^{48}Ca fusion reaction, Phys. Rev. C **76**, 011601(R) (2007).

[43] J. Dong, W. Zuo, J. Gu, Y. Wang, and B. Peng, α-decay half-lives and Q_α values of superheavy nuclei, Phys. Rev. C **81**, 064309 (2010).

[44] N. Wang, M. Liu, X. Wu, and J. Meng, Surface diffuseness correction in global mass formula, Phys. Lett. B **734**, 215 (2014).

[45] P. Möller, J. R. Nix, W. D. Myers, and W. J. Swiatecki, Nuclear ground-state masses and deformations, At. Data Nucl. Data Tables **59**, 185 (1995).

[46] J. Duflo and A. P. Zuker, Microscopic mass formulas, Phys. Rev. C **52**, R23 (1995).

[47] S. Goriely, N. Chamel, and K. M. Pearson, Further exploration of Skyrme-Hartree-Fock-Bogoliubov mass formulas. XII: Stiffness and stability of neutron-star matter, Phys. Rev. C **82**, 035804 (2010).

[48] E. L. Medeiros, M. M. N. Rodrigues, S. B. Duarte, and O. A. P. Tavares, Systematics of alpha-decay half-life: New evaluations for alpha-emitter nuclides, J. Phys. G **32**, B23 (2006).

[49] J. Khuyagbaatar *et al.*, ^{48}Ca + ^{249}Bk Fusion Reaction Leading to Element $Z = 117$: Long-Lived α-Decaying ^{270}Db and Discovery of ^{266}Lr, Phys. Rev. Lett. **112**, 172501 (2014).

[50] Y. Qian and Z. Ren, Half-lives of α decay from natural nuclides and from superheavy elements, Phys. Lett. B **738**, 87 (2014).